MICROSTRUCTURE EVOLUTION AND MECHANICAL RESPONSE IN THE HOT STAMPING PROCESS

AUTHORS:

Mats Oldenburg, Luleå University of Technology
Paul Åkerström, Gestamp Hardtech AB
Greger Bergman, Gestamp Hardtech AB
Per Salomonsson, Luleå University of Technology

CORRESPONDENCE:

Mats Oldenburg
Luleå University of Technology
Division of Solid Mechanics
SE-97187 Luleå
Phone +46 920 491752
Email mats.oldenburg@ltu.se

ABSTRACT

In the manufacturing of ultra high strength boron steel components with the hot stamping process, it is of great importance that the final product will have the desired material properties. This is especially true for safety related automotive components. Often the preferred microstructure is a mix of martensite and bainite. In this work a model is developed and implemented in order to predict the austenite decomposition into ferrite, pearlite, bainite and martensite during arbitrary cooling paths. The model is based on Kirkaldy's rate equations and later modifications by Li et al. After modification, the model accounts for the effect from the added boron and the effect of straining at high temperatures. The implementation is as part of a material subroutine in the finite element program LS-Dyna. The achieved volume fractions of micro-constituents and hardness profiles in the analyses show good agreement with the corresponding experimental observations. The phase content affect both the thermal and the mechanical properties during the process of continuous cooling and deformation of the material. A thermo-elastic-plastic constitutive model including effects from changes in the microstructure as well as transformation plasticity is implemented in the LS-Dyna code. The model is used together with a thermal shell formulation with quadratic temperature interpolation in the thickness direction. The developed methods are used to simulate the complete process of simultaneous forming and quenching of sheet metal components. The implemented models are used in coupled thermo-mechanical analysis of the hot stamping process and are evaluated by comparing the results from hot

stamping experiments. The results from simulations such as local thickness variations, hardness distribution and spring-back in the component show good agreement with experimental results. However, it is shown that the simulation of the final cooling stage relies on a correct modelling of contact properties and heat transfer.

KEYWORDS:

Hot stamping, phase transformations, mechanical response

INTRODUCTION

Simultaneous forming and quenching is a current manufacturing process for low weight and ultra high strength components. The process is often referred to as *hot stamping* or *press hardening* and is mainly used for producing safety related components for the automotive industry, such as side impact beams, bumper beams and different types of structural components.

The hot stamping process uses boron steel blanks which are first austenitized at a temperature of approximately 900 °C. The blank is then formed and quenched in cold tools to obtain martensitic ultra high strength material. The forming operation at elevated temperatures allows complex geometries to be obtained due to the high formability of the hot material.

The objective of the present work is to develop, improve and evaluate material related aspects in numerical simulations of the simultaneous forming and quenching process. The presented work focuses on the following aspects:

- Method development and determination of the flow stress of the austenite phase as a function of strain, strain rate and temperature.
- Austenite decomposition modelling and simulation for the actual steel grade.
- Constitutive modelling of the mechanical response by accounting for composite behaviour and transformation induced plasticity,
- Prediction of spring-back and distortion of the hot stamped component.

MODELLING OF HOT STAMPING

Compared to conventional cold forming there are numerous additional modelling and simulation aspects involved in the modelling, see Åkerström [1].

The blank, first heated to form austenite, is subsequently cooled by heat transfer to the tool parts and the austenite decomposes into different daughter phases. Depending on the temperature history and mechanical deformation, different phases and phase mixtures evolves. During the solid-state phase transformations, heat is released which influences the thermal field. Further, depending on the mixture of microconstituents, both the mechanical and thermal properties vary with temperature and deformation.

A realistic model used for the simulation of the simultaneous forming and cooling must consider interactions between the mechanical and temperature fields and the microstucture. The different fields and their interaction are shown in Figure 1, see Bergman [2]. Table 1 summarizes the different interactions with short descriptions.
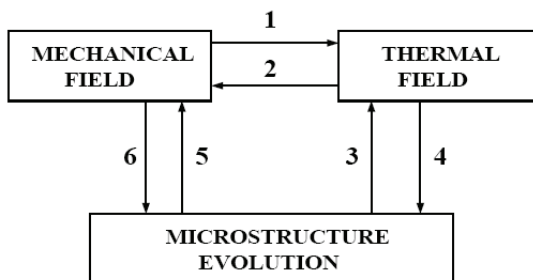

Figure 1: Interactions between the mechanical field, the thermal field and the microstucture evolution.

Table 1: Descriptions of interactions in figure 4, from [2].

No	Interaction Description
1a	Thermal boundary conditions are deformation dependent
1b	Heat generation due to plastic dissipation and friction (not accounted for in this work)
2	Thermal expansion
3a	Latent heat due to phase transformations
3b	Thermal material properties depend on microstructure evolution
4	Microstructure evolution depends on the temperature
5a	Mechanical properties depend on microstructure evolution
5b	Volume change due to phase transformations
5c	Transformation plasticity
5d	Memory of plastic strains during phase transformations
6	Phase transformations depend on stress and strain

In the simulation of hot stamping, shell elements is the natural choice when modelling the structural response of the workpiece/blank. In the hot stamping process, where the hot blank surfaces can be in both one-sided and double-sided contact with the tool as illustrated in Figure 2, the linear temperature approximation in the thickness direction is not accurate enough.

To accurately capture the heat transfer in this type of application, a thermal shell element with linear in-plane temperature approximation and quadratic in the thickness

direction is used. The theory for the linear-quadratic thermal shell element can be found in Bergman and Oldenburg [3].
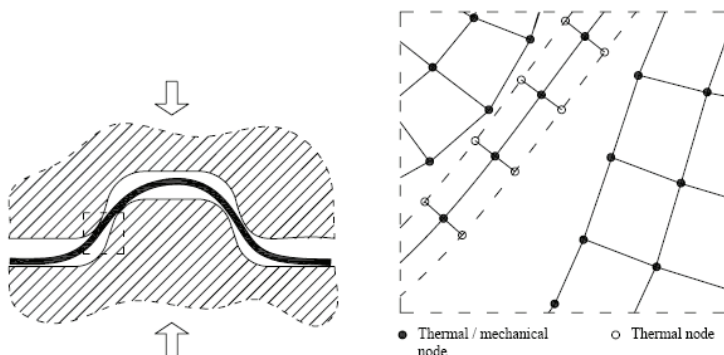

Figure 2: Principal configuration of the thermal shell element

Mechanical Material Modelling

The choice of constitutive equations and stress calculation algorithm will have a great impact on the predictive capabilities of the material model. However, the quality of the results achieved depends strongly on the stress-strain relationship used for the material. In the present work, improvements of the flow stress versus strain data for the austenite in the temperature interval 400-930 °C is presented.

Traditionally, the material is characterized by isothermal compression or tension tests at different temperatures. A drawback of the isothermal technique is the possibility of obtaining an increased amount of unwanted phases for some test temperatures and durations. An alternative approach is based on compression of cylindrical specimens at continuous cooling and different compression starting temperatures.

With the proposed method, the isothermal mechanical response is established by means of inverse modelling, see Åkerström et al. [4] and [5]. For the boron steel in the austenitic state, a physically based hardening function proposed by Nemat-Nasser [6] is found to describe the flow stress with good accuracy in the entire temperature range.

Modelling of Microstructural Evolution

The numerical simulations of the austenite decomposition into daughter phases and their compounds are based on Kirkaldys rate equations [7]. The models can be used to simulate the phase transformations without prior information from transformation diagrams. The diffusional transfor-mations (austenite to ferrite, pearlite or bainite) are predicted using these equations and the martensite evolution is modelled using the Koistinen and Marburger relation [8].
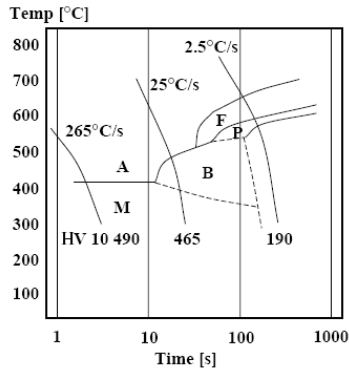
Figure 3: The manufacturer's CCT diagram for the Boron 02 steel.

The steel grade used in this work is boron steel produced by SSAB, with the trade name Boron 02. The specified alloy content is presented in Åkerström and Oldenburg [9]. The CCT diagram is shown in Figure 3.

The model proposed by Kirkaldy and Venugopalan in [7] is used in a slightly modified form. The set of equations which model the austenite decomposition can all be written in a general form as

$$\frac{dX_i}{dt} = f(G)f(C)f(T)f(X_i) \tag{Eq.1}$$

where f indicates a general functional relation. In Eq. (1), $f(G)$ is the effect of the austenite grain size, $f(C)$ the effect of alloy composition, $f(T)$ is a function of temperature and $f(X_i)$ gives the effect of current fraction formed. Details of the implementation can be found in [9]. The transformation from austenite to martensite is modelled using the relation proposed by Koistinen and Marburger [8], which is formulated as

$$X_m = X\gamma(1 - e^{-\alpha(M_s - T)}) \tag{Eq.2}$$

In Eq. (2), X_m is the volume fraction martensite, and $X\gamma$ is the volume fraction of austenite. The factor α is equal to 0.011 for many steels and $(M_s - T)$ is the supercooling below the martensite start temperature, M_s. As has been shown in Somani et al. [10], straining the austenite at high temperatures will change the austenite decomposition kinetics so that ferrite will form earlier in time. In the current model, the ferrite reaction kinetics has been modified according to Serajzadeh [11].

Composite Behaviour and Transformation Plasticity

The present model, based on the model proposed by Leblond et al. in [12], and Leblond in [13], start from the behaviour of each phase and works back to the macroscopic behaviour of the material. The yield stress, $^{t+\Delta t}\sigma^y$, is represented by a linear mixture law as

$$^{t+\Delta t}\sigma^y = {}^t\sigma^y + \sum_{k=1}^{5} {}^{t+\Delta t}X_k \, {}^{t+\Delta t}H_k \Delta\bar{\varepsilon}_k^p \tag{Eq.3}$$

where $^{t+\Delta t}\sigma^y$ is a function of the volume fraction and the effective plastic strains of the individual phases as well as the temperature. In Eq. (5), $^{t+\Delta t}X_k$ is the known volume fraction of phase k, $^t\sigma^y$ is the yield stress corresponding to the known effective plastic strains $^t\bar{\varepsilon}_k^p$, the current temperature $^{t+\Delta t}T$ and $^{t+\Delta t}H_k$ which is the current plastic modulus for phase k. Multi piecewise linear representation of the true stress versus effective plastic strain is used.

A commonly used model for transformation plasticity based on the Greenwood-Johnson mechanism [14] is the model by Leblond and coworkers, see e.g. [12]. The implementation of the model is described in detail in Åkerström et al. [15].
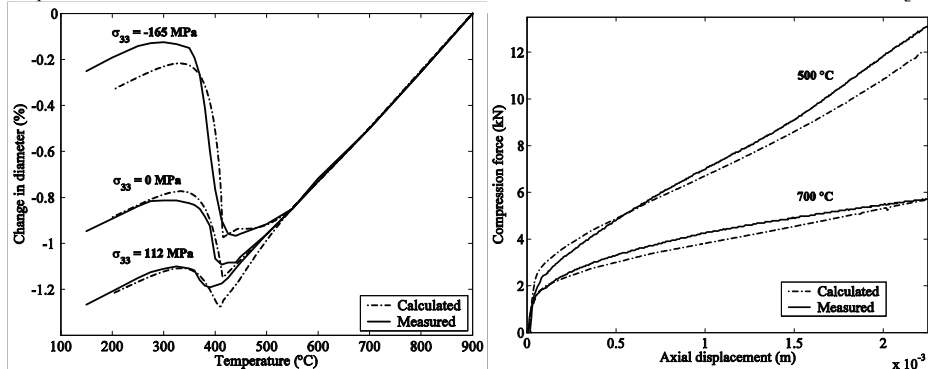

Figure 4a: Change in diameter as a function of temperature and axial stress on a cylindrical specimen. 4b: Compression force versus axial displacement at the temperatures 500 and 700 °C.

Figure 4a shows the measured and calculated change in diameter for a loaded and unloaded cylindrical specimen when accounting for TRIP, from [15], and Figure 4b shows measured and calculated responses from iso-thermal compression.

HOT STAMPING EXPERIMENT

The experimental tool consists of two main parts, an upper punch and a lower die shown in Figure 5. The tools will produce a component with a hat section with a height of 0.052 m (length 0.140 m), that after a transition zone becomes flat, see [1]. The final length of the component is 0.250 m.

Four small spring supported pins are mounted at the top of the die to prevent the hot blank to come into tool contact during the blank insertion phase. The material used in the tools is SS2242-02, manufactured by Uddeholm AB, see [1]. The 3D finite element mesh of the tool parts consists of a total of 57399 eight node brick elements, see Figure 6.
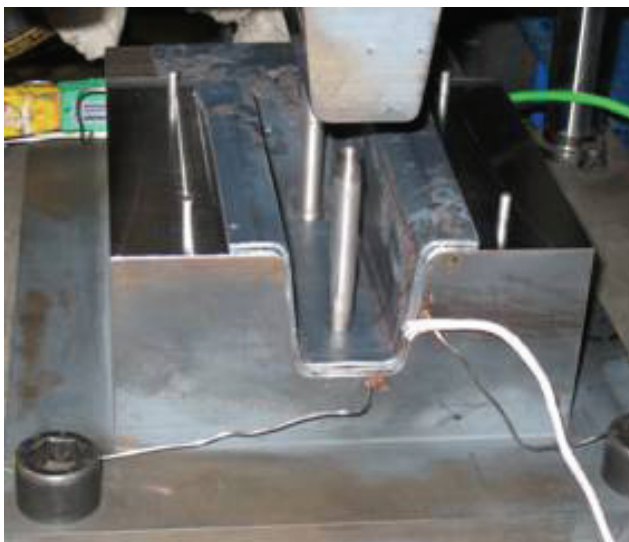

Figure 5: Tools and the shape of the final component, from [1].

RESULTS FROM EXPERIMENT AND ANALYSIS

Measured and calculated forming forces are shown in Figure 7a. Note that the calculated forming force exhibits some oscillations at the first part of the curve. The oscillations are due to the dynamics response when the punch hits the blank.

The final shape is measured at different cross sections of the component, see [1] Only a small spring-back in the component is expected from the hot stamping process. In Figure 7b, the final calculated and measured geometry, at a cross-section 0.225 m from the hat shaped side, is presented.
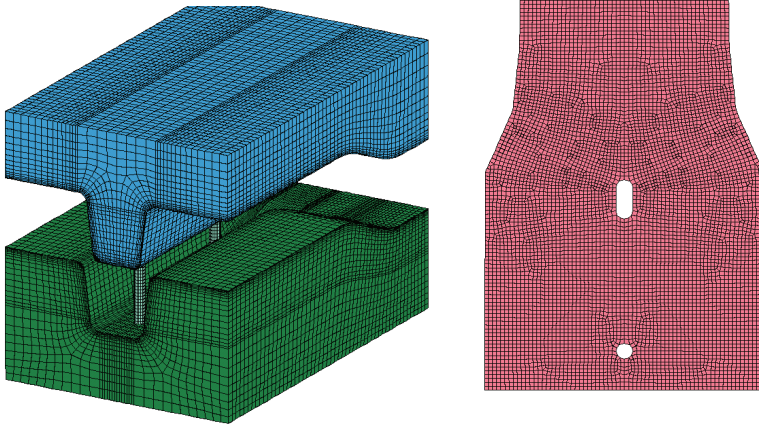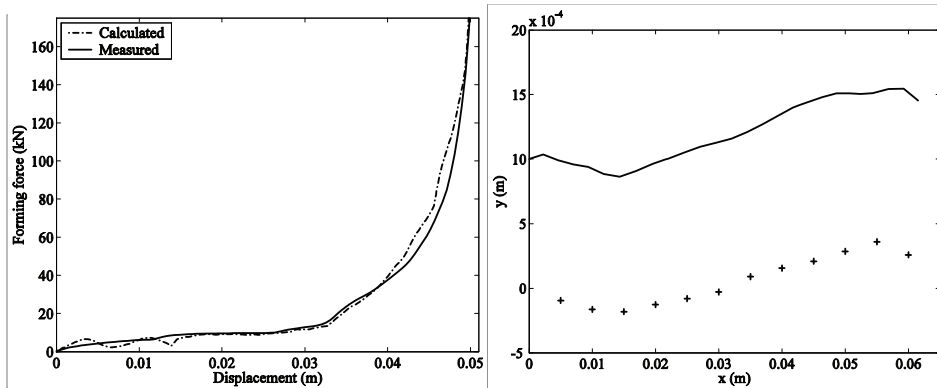
Figure 6: FE-model of blank and tools.

Figure 7a: Measured and calculated forming force as function of punch displacement. 7b: Final shape at 0.225 m from the hat-shaped side of the component. The solid lines is the calculated at mid-surface and crosses are measured points on lower tool side (approximately 1 mm offset).

The measured and calculated minimum thickness in this area are $1.65 \cdot 10^{-3}$m and $1.63 \cdot 10^{-3}$m, respectively. The measured and calculated maximum thickness are $2.18 \cdot 10^{-3}$m and $2.26 \cdot 10^{-3}$m, respectively.
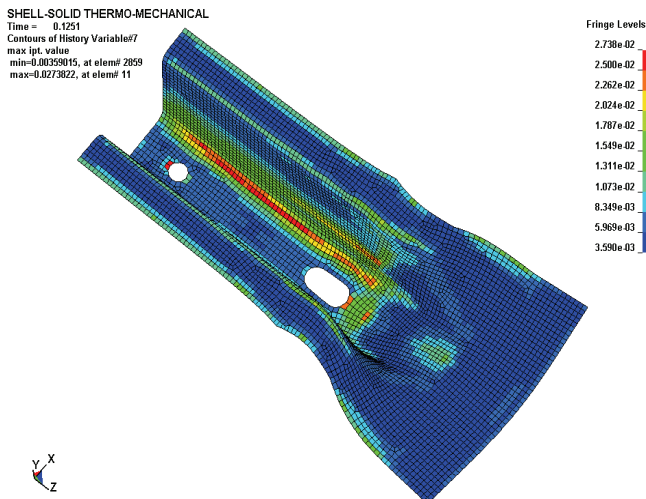
Figure 8: Calculated volume fractions of ferrite for a hot stamped component.

The distributed phase content in the component and associated distributed mechanical properties of the final component can be obtained from the analyses. In Figure 8 the final maximum ferrite distribution in the component is shown, the maximum value is 2.78 % and is found in the parts of the component subjected to straining at high temperature. From different tests with displacement and force controlled analyses it is clear that the analyses with respect to the phase content are rather sensitive to that correct boundary conditions are imposed during the process. For example, the analysis presented above was displacement controlled, resulting in to large contact areas between the tools and the component. The maximum ferrite content from an analysis with force control was 5.45 %. In this case it is expected that the contact areas are more correctly represented in the analysis.

CONCLUSIONS AND DISCUSSION

The presented work includes the modelling of the major phenomena involved in hot stamping. In the resulting model, most of the couplings between the thermal and the mechanical fields are present. The mechanical properties, represented by the nonlinear hardening law valid for large strains, of each phase are accounted for in a linear mixture law. The mechanical properties of the austenite phase are obtained by inverse modelling of multiple continuous cooling and deformation tests allowing for accurate experiments within the 10 seconds available for testing without obtaining influence from unwanted phases. The forming of austenite is dominating the mechanical response. However, one goal for the future is to perform similar studies involving the ferrite, pearlite and bainite phases in order to obtain more accurate material descriptions.

The current work together with [2] is intended to improve and facilitate the design and development of ultra high strength components with the hot stamping technique. It has been shown that the used models can give accurate predictions of the hot stamping process, both for the phase transformations and for the mechanical response. One objective of the present work is to evaluate the shape deviations after the forming process is finished. It is concluded that the model can predict thickness variations and final shape with good accuracy.

REFERENCES

1. P. Åkerström, "Modelling and simulation of hot stamping", PhD. Thesis 2006:30, Luleå university of technology, 2006.
2. G. Bergman, "Modelling and simultaneous forming and quenching". PhD. Thesis, Luleå University of Technology, 1999.
3. G. Bergman and M. Oldenburg, *Int. J. Numer. Meth. Eng.* **59**, 1167–1186 (2004).
4. P. Åkerström, B.Wikman and M. Oldenburg, *Modelling Simul. Mater. Sci. Eng.* **13**, 1291-1308 (2005).
5. P. Åkerström and M. Oldenburg, *J. Phys. IV* **120**, 625-633 (2004).
6. S. Nemat-Nasser, "Experimental-based micromechanical modelling of metal plasticity with homogenisation from micro- to macro-scale properties" in *IUTAM symposium on micro- and macro structural aspects of thermo plasticity* edited by O.T. Bruhns and E. Stein, Kluwer academic publishers, 1999, pp. 101–113.
7. J.S. Kirkaldy and D. Venugopalan, "Prediction of microstructure and hardenability in low alloy steels" in *International Conference on Phase Transformations in Ferrous Alloys*, edited by A.R. Marder and J.I. Goldstein, Philadelphia, 1983, pp. 125–148.
8. D.P. Koistinen, R.E. Marburger, *Acta Metall.* **7,** 59–60 (1959).
9. P. Åkerström and M. Oldenburg, *Journal of Materials Processing technology* **174**, 399-406 (2006).
10. M.C. Somani, L.P. Karjalainen, M. Eriksson and M. Oldenburg, *ISIJ International*, **41**, 361–367 (2001).
11. S. Serajzadeh, *Journal of Materials Science and Engineering* **146**, 311–317 (2004).
12. J.B. Leblond, G. Mottet and J.C. Devaux, *J. Mech. Phys. Solids* 34, 395–409 (1986).
13. J.B. Leblond, *International Journal of Plasticity* **5**, 573–591 (1989).
14. G. W. Greenwood and R. H. Johnson, *Proc. Royal Society* **283**, 403–422 (1965).
15. P. Åkerström, G. Bergman and M. Oldenburg, , Modelling Simul. Mater. Sci. Eng. **15** (2007) 105–119